Desalination 404 (2017) 322–327

Contents lists available at ScienceDirect

Desalination

journal homepage: www.elsevier.com/locate/desal

Preparation of POSS-derived robust RO membranes for water desalination

Kazuki Yamamoto [a], Sayako Koge [a], Takahiro Gunji [b], Masakoto Kanezashi [c], Toshinori Tsuru [c,*], Joji Ohshita [a,*]

[a] Department of Applied Chemistry, Graduate School of Engineering, Hiroshima University, Higashi-Hiroshima 739-8527, Japan
[b] Department of Pure and Applied Chemistry, Tokyo University of Science, Noda 278-8510, Japan
[c] Department of Chemical Engineering, Graduate School of Engineering, Hiroshima University, Higashi-Hiroshima 739-8527, Japan

HIGHLIGHTS

- POSS-derived membranes were prepared.
- The POSS-derived membranes had high liquid permeance and NaCl rejection of 1×10^{-13} m/s·Pa and 90%, respectively.
- At 90 °C, water permeance increased to approximately 1×10^{-12} m/s·Pa with NaCl rejection remaining nearly unchanged.
- The membranes exhibited tolerance to 1×10^{4} ppm·h chlorine exposure.

GRAPHICAL ABSTRACT

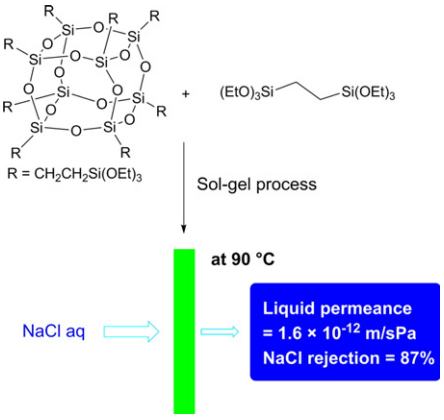

ARTICLE INFO

Article history:
Received 30 July 2016
Received in revised form 1 October 2016
Accepted 7 November 2016
Available online 24 November 2016

Keywords:
POSS-containing membrane
Reverse osmosis
Water desalination
Thermal stability
Chlorine resistance

ABSTRACT

POSS (polyhedral oligomeric silsesquioxane)-containing silica sols were prepared by hydrolysis/condensation of octakis(triethoxysilylethyl)-substituted POSS (TESE-POSS) and mixtures of 1,2-bis(triethoxysilyl)ethane (BTESE1) and TESE-POSS in HCl/H_2O/EtOH. Nitrogen adsorption isotherms of bulk gels prepared by drying the sols indicated that the gels had porous properties with surface areas of 168–424 m^2/g, depending on the BTESE1/TESE-POSS molar ratio. The sols were coated on $SiO_2/ZrO_2/TiO_2$ porous supports and calcinated at 350 or 400 °C to produce the membranes. Water desalination performance of the membranes was evaluated by reverse osmosis (RO) experiments using 2000 ppm NaCl aqueous solution. At 25 °C, liquid permeance was approximately 1×10^{-13} m/s·Pa and NaCl rejection was 90%. Interestingly, the membranes were robust to heat and chlorine. Membrane performance was not changed even after exposure of the membranes to as high as 1×10^{4} ppm·h aqueous NaOCl. When RO experiments were conducted at 90 °C, liquid permeance was increased to approximately 1×10^{-12} m/s·Pa whereas NaCl rejection remained nearly unchanged, indicating potential application of the membranes to high-temperature water separation. Lowering the operation temperature again to 25 °C resulted in the recovery of the original data, indicating that the membranes were neither decomposed nor damaged upon contact with hot water.

* Corresponding authors.
E-mail address: jo@hiroshima-u.ac.jp (J. Ohshita).

http://dx.doi.org/10.1016/j.desal.2016.11.017
0011-9164/

1. Introduction

Silica membranes that are typically prepared by hydrolysis/condensation, the so-called sol-gel process of tetraethoxysilane, have been well studied for gas separation [1–5]. Their dense structures allow for the separation of small molecules, such as He, H_2, and N_2. However, silica membranes are usually too dense for use in water separation [4,5]. In addition, silica materials composed of only Si—O linkages are not stable towards hydrolysis and thus cannot be used as water separation membranes with long operating lifetimes [6–8]. It was reported that the introduction of ethylene bridges by employing 1,2-bis(triethoxysilyl)ethane (BTESE1 in Chart 1) as the precursor expands the Si—O network to enhance porosity, thereby improving water permeability [9]. Thus, BTESE1-based membranes, which have approximately 1×10^{-13} m/s·Pa water permeance and >95% NaCl rejection, can be used as reverse osmosis (RO) membranes. It was also demonstrated that the bridged silica membranes are robust to chlorine and high-temperature operation. Thereafter, many organic bridges have been developed to investigate structure-performance relationships [10–14], and the introduction of sterically more rigid bridges, such as ethenylene and ethynylene (BTESE2 and BTESE3 in Chart 1), has further expanded the networks, improving water permeance to 2×10^{-13} m/s·Pa and 8×10^{-13} m/s·Pa, respectively [10,11]. The polarity of the ethenylene and ethynylene bridges also affects membrane hydrophilicity and thus enhances water permeability. However, Si—C (sp^2) and Si—C (sp) bonds are usually less stable than Si—C (sp^3) bonds towards acid and alkali treatment and exposure to chlorine [12,15]. Membranes with more polar triazine units were also prepared by the tris(triethoxysilylpropoxyl)triazine sol-gel process and demonstrated high performance for water separation. However, the precursor was difficult to handle because of its strong tendency to undergo hydrolysis even with atmospheric moisture, in which the highly basic triazine unit was likely to work as a self-catalyst for the hydrolysis [16].

On the other hand, POSS (polyhedral oligomeric silsesquioxane, T8)-derived membranes are known to possess high porosity [17–20]. The hydrolysis/condensation polymerization of highly rigid and cubic POSS compounds with multiple reactive sites does not produce regularly packed structures, but proceeds randomly to give an amorphous network with intercubic pores. For example, the alkali-catalyzed polymerization of octahydro-POSS (H-POSS in Chart 1) yielded membranes with the average pore size of 0.42 nm when the sol was calcinated on an inorganic $SiO_2/ZrO_2/TiO_2$ support at 550 °C [17,18]. Their applications to gas separation were also explored.

In the present work, we introduced a (triethoxysilyl)ethyl group to each corner silicon of POSS (TESE-POSS in Chart 1) and subjected it to hydrolysis to form POSS-bridged silica membranes for water separation. Co-polymerization of TESE-POSS with BTESE1 was also carried out to determine the influence of POSS incorporation on the separation properties of the membranes. The performance of the membranes was examined in RO experiments using 2000 ppm NaCl aqueous solution. The robustness of the membranes to chlorine and heat was also investigated.

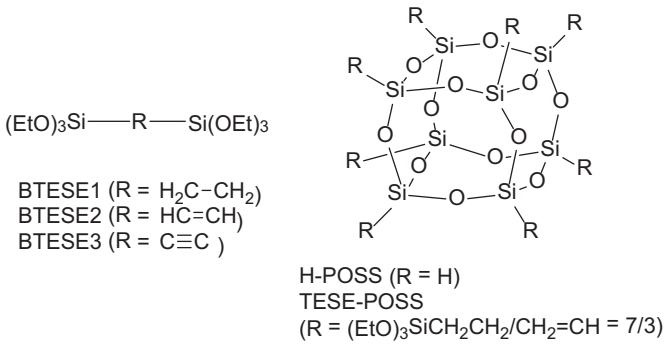

Chart 1. Structures of bridged silica precursors.

2. Experimental

2.1. General

Octavinyl-substituted POSS was obtained as reported in the literature [21]. NMR spectra were recorded on a Varian System 500 spectrometer. Dynamic light scattering (DLS) analysis of the POSS-containing sols was carried out in ethanol solution using a Malvern Zetasizer Nano (Malvern, ZEN3600) analyzer. IR spectra were obtained on a Shimadzu IRAffinity-1 spectrometer using thin films coated on silicon wafer. Thermogravimetric analysis (TGA) was performed on a SII EXSTAR TG-DTA6200 thermal analyzer from 100 °C to 1000 °C at the heating rate of 10 °C/min, after heating the sol samples at 60 °C for 30 min to remove the solvents. Water contact angle measurements were performed on a Kyowa DM300 contact angle meter. Nitrogen adsorption was measured using MicrotracBEL Corp. Belsorp-Max instrument and BET surface areas (S_{BET}) were estimated from the nitrogen adsorption isotherms. Pencil hardness tests of the film surface were carried out according to the ASTM Standard D 3363–92 [22], using a BEVS1301 Pencil Tester (BEVS). Liquid conductivities were measured on a HORIBA ES-51 conductivity meter.

2.2. Preparation of TESE-POSS

A mixture of octavinyl-substituted POSS (0.500 g, 0.790 mmol), triethoxysilane (1.25 g, 7.61 mmol), Karstedt's catalyst (37.8 μL, 1.69×10^{-3} mmol), and THF (40 mL) was stirred at room temperature under a dry argon atmosphere for 5 h. After removal of the solvent, the residue was purified by preparative GPC (gel permeation chromatography) to provide 0.29 g (25% yield) of the title compound. NMR analysis revealed that approximately 88% of the vinyl units had been hydrosilylated. ^{1}H NMR (δ in $CDCl_3$) 0.65 (t, 28H, ethylene), 1.22 (t, 63H, CH_3 of ethoxy), 3.81 (q, 42H, CH_2 of ethoxy), 6.0–5.8 (m, 3H, vinyl); ^{13}C NMR (δ in $CDCl_3$) 1.65, 3.43, 18.28, 58.34; ^{29}Si NMR (δ in $CDCl_3$) -66.82, −45.68.

2.3. Sol-gel process

To a solution of 0.25 g of TESE-POSS or BTESE1/TESE-POSS in 4.6 g of EtOH was slowly added 0.38 mL of 0.1 M HCl (aq). The mixture was stirred for 2–5 h at room temperature until the sol particle size determined by DLS analysis exceeded 2 nm (Figs. 1 and S1–3). The mixture was then diluted with ethanol to 0.25 wt% (based on the amount of starting alkoxysilanes) and stored in a refrigerator (4 °C) until use. The sol was heated at 60 °C in a glass vial to yield a gel powder for the nitrogen adsorption isotherm measurement, and was cast-coated on silicon wafer and heated to give a gel film for IR spectrometry. Water contact

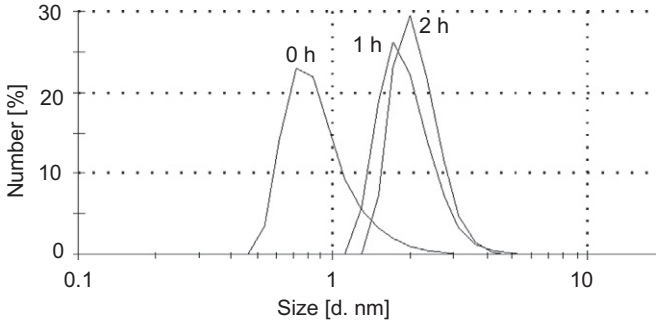

Fig. 1. DLS profiles of TESE-POSS homo-polymer sols immediately after mixing in the reaction medium, and after 1 and 2 h reaction.

angle measurements were performed using gel films similarly prepared on silicon wafer, and calcinated at 350 °C and 400 °C for TESE-POSS and BTESE1/TESE-POSS gels, respectively.

For the membrane preparation, an alumina tubular porous support (average pore size = 150 nm, outer diameter = 3 mm, length = 50 mm) was coated five times with 0.72 wt% aqueous TiO_2 (average particle size = 30 nm), and then three times with 0.25 wt% aqueous SiO_2-ZrO_2 (Si/Zr = 1, average particle size = 50 nm) to form an intermediate layer. After each coating, the tubular substrate was heated at 550 °C for 15 min in air. At this stage, the average pore size of the intermediate layer was estimated to be <2 nm by nanopermporometry [23,24]. Finally, the separation layer was prepared by coating TESE-POSS or BTESE1/TESE-POSS sol on the intermediate layer, followed by calcination at 350 °C or 400 °C, respectively, in nitrogen.

2.4. RO experiments

RO experiments were carried out using 2000 ppm NaCl aqueous solution at 25 °C and the feed pressure of 1.0 MPa applied by a plunger pump. Liquid permeance (L_p) and NaCl rejection (R) were calculated using equations (1) and (2), respectively (ΔP = difference in applied pressure, $\Delta\pi$ = osmotic pressure, Jv = permeate water flux, and C_f and C_p = NaCl concentrations of feed and permeate determined from their conductivities). In this study, concentration polarization is negligible because of low water flux ($<10^{-7}$ m/s) and mass transfer coefficient ($<10^{-5}$) [25,26]. Also, electroviscosity was not considered because it was reported that water flux was not changed by using different solutes in aqueous solution in case of using similar organosilica-based membrane [27]. Details of the RO experiments are given in the literature [9].

$$L_p = J_v/(\Delta P - \Delta\pi) \quad (1)$$

$$R = (1 - C_p/C_f) \times 100 \quad (2)$$

2.5. Stability test of the membrane towards chlorine exposure

The membrane was immersed in 100 ppm NaOCl aqueous solution in the dark at room temperature with pH being adjusted to 7 using 0.2 M KH_2PO_4 buffer. After every 20 h, the membrane was thoroughly rinsed with deionized water and subjected to the RO experiment as described above.

3. Results and discussion

3.1. Sol and membrane preparation

The precursor TESE-POSS was prepared by Pt-catalyzed hydrosilylation of octavinyl-POSS with triethoxysilane. This reaction did not proceed to completion and approximately 88% of the vinyl groups were converted into triethoxysilylethyl units, likely due to steric congestion. For the sol preparation, TESE-POSS was hydrolyzed with water in ethanol in the presence of a catalytic amount of HCl at room temperature, and the progress of the reaction was monitored by DLS analysis. Immediately after TESE-POSS was dissolved in the mixed solvent of HCl/H_2O/EtOH at room temperature, DLS analysis revealed the formation of particles measuring approximately 0.7 nm in size. The particle size increased to approximately 2 nm after stirring the mixture for 1 h, as shown in Fig. 1. Co-polymerization with BTESE1 in three different BTESE1/TESE-POSS molar ratios = 1, 4, and 8 was also found to yield the corresponding sols with particle sizes of 1–2 nm, as presented in Figs. S1–S3. For the membrane preparation, sols with sizes larger than 2 nm were coated on the $SiO_2/ZrO_2/TiO_2$ intermediate layer, whose average pore size was <2 nm, and the sol films were calcinated.

It is common knowledge that a higher calcination temperature leads to better separation selectivity as network densification is enhanced. Heating the gel at a high temperature, however, may induce thermal degradation of the organic framework. To determine the calcination temperature, we investigated the thermal stability of the gels. Fig. 2 presents the results of thermogravimetric analysis (TGA) of gel powders that were prepared by drying the homo- and co-polymer sols at 60 °C for 30 min. We also measured the IR spectra of the gel films prepared by spin-coating the sols on silicon wafer, followed by heating the coated wafer in nitrogen. The spectra of TESE-POSS and BETSE1/TESE-POSS = 4 gel films after heating the films at different temperatures are shown in Fig. 2.

For the homo-polymer gels, weight loss proceeded in two steps in TGA. The weight loss at 250–350 °C is likely ascribed to the dehydration of the remaining Si—OH groups and the decomposition of Si-OEt to form Si—OH that also undergoes dehydration, whereas that at 420–600 °C seems to indicate the decomposition of the ethylene units attached to the POSS corners [18]. In accordance to the TGA profile, the signal at approximately 900 cm^{-1} in the IR spectra, which was ascribed to Si—OH stretching [28], was gradually weakened and finally disappeared when the sol film was treated at 300 °C (Fig. 3a). Two types of C—H stretching bands were observed at approximately 2970 cm^{-1} and 2880–2930 cm^{-1} in the IR spectrum of the gel dried at 100 °C, which were ascribed to CH_3 (ν_{as}) and CH_3 (ν_s)/CH_2 ($\nu_s + \nu_{as}$), respectively. The former was weakened from 200 °C, whereas the latter showed an obvious decrease starting at 300 °C, suggesting that the decomposition of the ethoxy group occurred at a lower temperature than that of the ethylene bridges.

For the co-polymers, we observed much lesser weight loss, as shown in Fig. 2. Although the mechanism is not clearly understood yet, the incorporation of small BTESE1 molecules would enhance network formation, which would improve the thermal stability of the gels. TGA showed weight loss ascribed to dehydration and EtO decomposition at 200–500 °C and that attributable to ethylene decomposition in the temperature range of 550–650 °C, which was slightly higher than the ethylene decomposition temperature range of the homo-polymer gel. The IR spectra in Fig. 3b changed depending on the heating temperature, similarly to those of the TESE-POSS-derived gel. From these observations, we determined that the calcination temperatures were 350 °C and 400 °C for homo- and co-polymer membranes, respectively.

Then, we estimated the porosity of the gel powders by nitrogen adsorption isotherm measurement at 77 K. As presented in Fig. 4, the gels prepared by homo-polymerization of TESE-POSS and co-polymerization in BTESE1/TESE-POSS molar ratio = 1 showed a type-I profile, similar to that reported for the BTESE1-derived gel. Type-II profiles were seen for

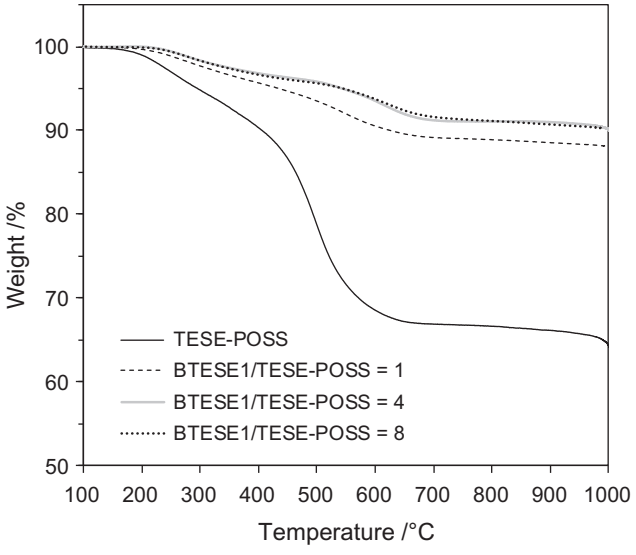

Fig. 2. TGA profiles of POSS-containing polymer gels in nitrogen.

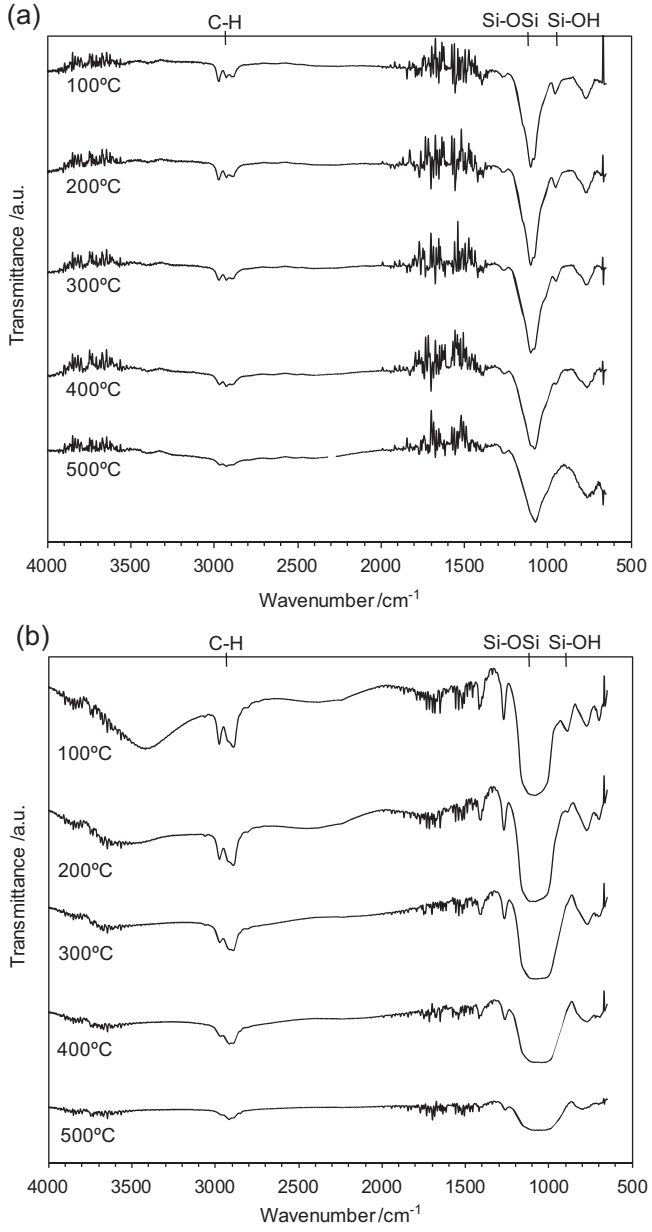

Fig. 3. IR spectra of homo- (a) and 4:1 co-polymer (b) gel films after heating at different temperatures.

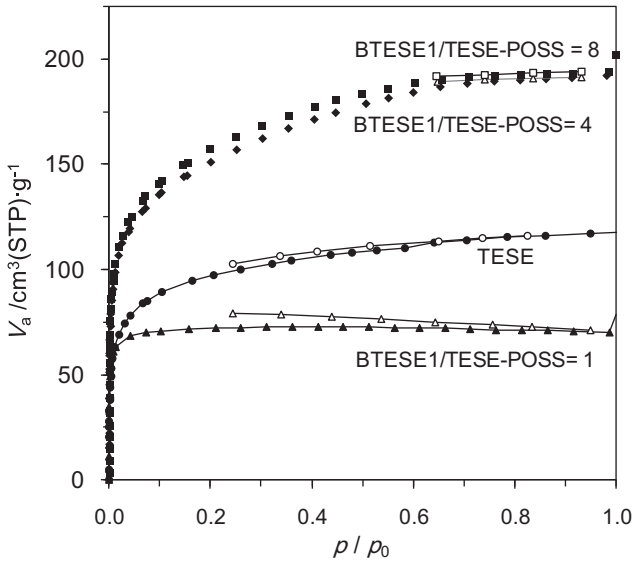

Fig. 4. Nitrogen adsorption isotherms of POSS-containing gels.

co-polymer gels with BTESE1/TESE-POSS molar ratios = 4 and 8, suggesting the existence of mesopores. The BET surface areas of the co-polymer gels (ca. 400 m^2/g) were higher than that of BTESE1-derived gel (343 m^2/g), except for the co-polymer gel prepared in BTESE1/TESE-POSS molar ratio = 1, whose surface area was determined to be 168 m^2/g, as listed in Table 1.

Membrane hydrophilicity is also an important factor for applications to water separation, and higher hydrophilicity usually results in better water permeability. Water contact angles were measured for the gel films prepared by coating the sols on silicon wafers, followed by heating in nitrogen at the calcination temperature determined as above. As summarized in Table 1, water contact angles larger than 80° were obtained for all the gel films, indicating low hydrophilicity. Interestingly, hydrophilicity was improved as the BTESE1 incorporation ratio was increased. The mechanical strength of the gel film surfaces was also examined by the pencil hardness test. Increasing the BTESE1 incorporation ratio tended to decrease film hardness; nevertheless, all the film surfaces had sufficiently high mechanical strength. The results of the pencil hardness test are also summarized in Table 1.

3.2. RO experiments

Separation membranes were prepared by coating the sols on SiO_2/ZrO_2/TiO_2 substrates, followed by calcination in nitrogen at 350 °C and 400 °C for the homo- and co-polymers, respectively, as described in the Experimental section. For the co-polymer, the BTESE1/TESE-POSS molar ratio of 4 was employed, because the gel prepared in this ratio had the maximal surface area. RO experiments were carried out using 2000 ppm NaCl aqueous solution at 1.0 MPa and 25 °C, and liquid permeance and NaCl rejection were determined, as summarized in Table 2. The homo-polymer-based membrane exhibited higher NaCl rejection and lower permeance than the co-polymer-based one. As listed in Table 2, POSS-derived membranes showed slightly lower NaCl rejection than most of other bridged silica membranes reported previously [9–13]. However, liquid permeance of the membrane with BTESE1/TESE-POSS = 4 was higher than or comparable to those of other

Table 1
Properties of POSS-containing gels.

Monomer	$S_{BET}/(m^2/g)$	Water contact angle/°	Pencil hardness test
TESE-POSS	394	89	>6H
BTESE1 /TESE-POSS = 1	168	84	5H
4	424	82	>6H
8	409	80	>6H
BTESE1[a]	343	63	>6H

[a] Reference 28.

Table 2
Water desalination performance of POSS-containing membranes at 25 °C, in comparison with that of other organosilica membranes reported previously.

Monomer	Liquid permeance/(m/s·Pa)	NaCl rejection/%
TESE-POSS	7.6×10^{-14}	88
BTESE1/TESE-POSS = 4	1.4×10^{-13}	86
BTESE1 [9]	1×10^{-13}	98
BTESE2 [10]	2×10^{-13}	98
BTESE3 [11]	8×10^{-13}	95
BTESNor [12]	6.3×10^{-14}	95
BTESMOU [13]	9.0×10^{-14}	85

membranes, except for BTESE3-derived membrane that showed approximately 5 times higher liquid permeance. To explore the robustness of the membranes, we examined how robust the membranes are to chlorine and heat. The membranes were immersed in 100 ppm NaOCl aqueous solution and separation performance was examined after every 20 h. As shown in Fig. 5, no obvious changes were seen up to the exposure time of 100 h (chlorine exposure = 10,000 ppm·h), indicating high tolerance of the membranes towards chlorine exposure. To investigate the robustness of the membranes to heat, RO experiments were carried out using hot NaCl solution (2000 ppm) (Fig. 6). Elevating the solution temperature to 90 °C increased liquid permeance to approximately 9.0×10^{-13} m/s·Pa and 1.6×10^{-12} m/s·Pa for the homo- and co-polymer-based membranes, respectively. Those values were approximately 11–12 times larger than the values at 25 °C. On the other hand, no significant changes were observed for NaCl rejection. Upon cooling the liquid temperature again to 25 °C, the original performance was recovered, indicating that neither damage nor decomposition of the membranes occurred during the high-temperature operation. Similar robustness of BTESE1-derived membranes has been reported [9]. Although liquid permeance of the BTESE1-derived membrane at 25 °C was slightly higher than those of the present membranes,

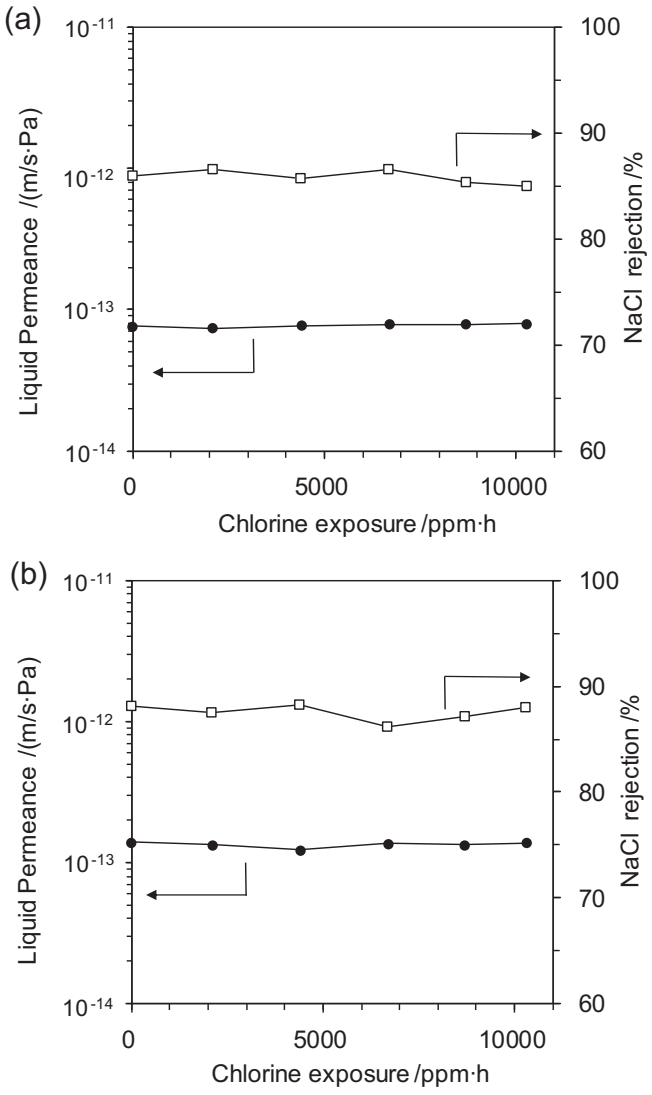

Fig. 5. Effects of chlorine exposure on liquid permeance and NaCl rejection of homo- (a) and co-polymer (BTESE1/TESE-POSS molar ratio = 4) membranes, using 100 ppm NaOCl solution.

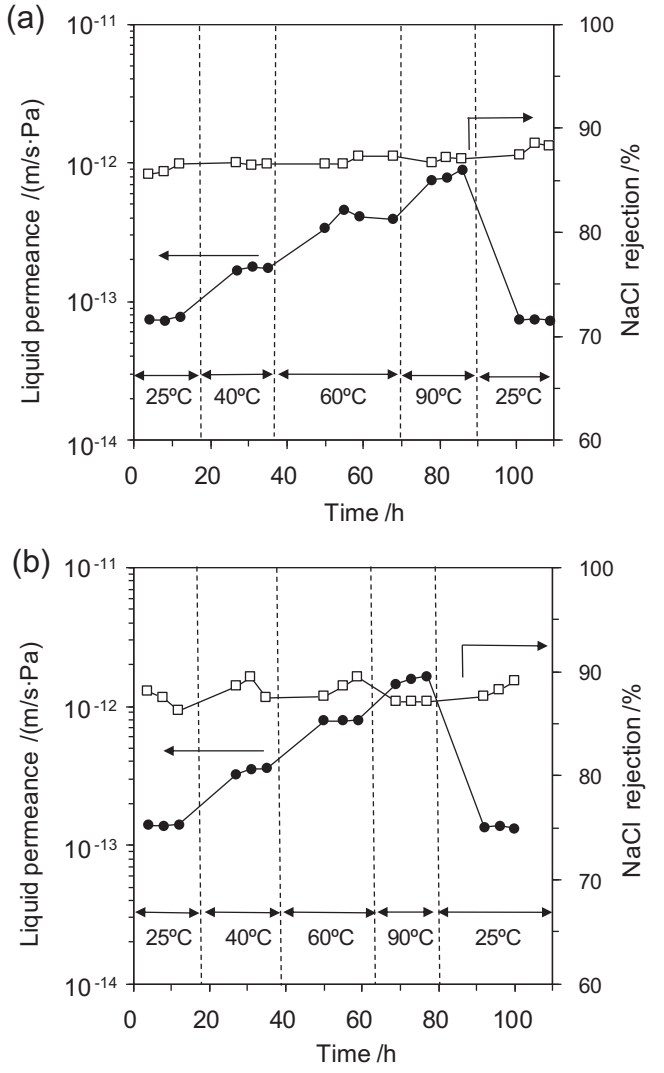

Fig. 6. Plots of liquid permeance and NaCl rejection of homo- (a) and *co*-polymer (BTESE1/TESE-POSS molar ratio = 4) membranes versus operation period, using 2000 ppm NaCl solution at 25–90 °C.

liquid permeance at 90 °C was 9.0×10^{-13} m/s·Pa, which was comparable to or lower than those of the present membranes.

Temperature dependence of liquid permeance of aqueous solutions is well correlated by an Arrhenius plot [29], given as the following equitation, where L_p is the liquid permeance, A_p is the frequency factor, and E_p is the activation energy of permeation, respectively.

$$L_p = A_p \exp(-E_p/RT) \quad (3)$$

Arrhenius plots of liquid permeance are shown in Fig. 7. Activation energy of TESE-POSS, TESE-POSS/BTESE1, and BTESE1 membrane were calculated to be 32.8, 33.1, and 27.4 kJ/mol, respectively. The higher activation energies for POSS-containing membranes than that of BTESE1 is ascribed to the long linker ethylene-POSS-ethylene unit between the triethoxysilyl groups. The thermal vibration of the flexible linker would enhance the water permeability to larger extents than BTESE1-based membrane, being responsible for their high liquid permeability at high temperature.

4. Conclusions

We successfully prepared POSS-containing membranes by homopolymerization of TESE-POSS and co-polymerization of BTESE1/TESE-

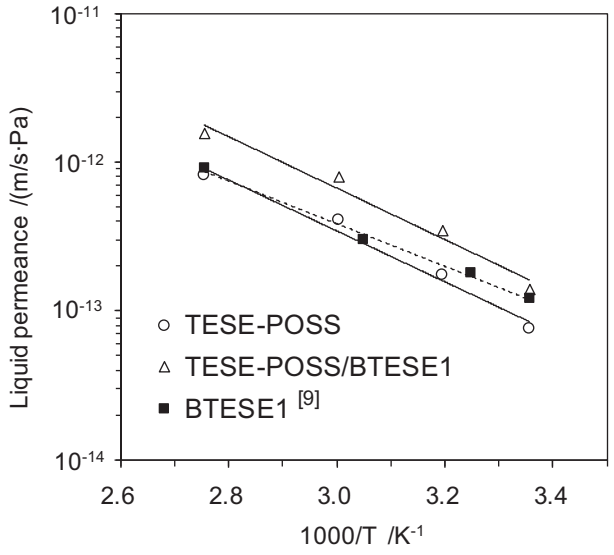

Fig. 7. Arrhenius plot of the liquid permeance by the temperature dependence.

POSS. The membranes showed higher BET surface areas than the BTESE1-based membrane. RO experiments revealed that the membranes showed water separation properties and were robust to chlorine and heat. The co-polymer membrane with BTESE1/TESE-POSS molar ratio = 4 showed liquid permeance at 90 °C, which was 1.8 times higher than that reported for the BTESE1-based membrane, suggesting its potential use as separation membrane for high-temperature operation, although NaCl rejection was slightly lower than that of the BTESE1-based membrane.

Acknowledgements

This research was supported by the project "Development of Robust RO/NF Membranes for Various Types of Water Resources" of the Core Research for Evolutional Science and Technology, Japan Science and Technology Agency (CREST, JST).

Appendix A. Supplementary data

Supplementary data to this article can be found online at http://dx.doi.org/10.1016/j.desal.2016.11.017.

References

[1] A. Darmawan, J. Motuzas, S. Smart, A. Julbe, J.C.D. da Costa, J. Membr. Sci. 474 (2015) 32–38.
[2] J. Wang, Y. Li, Z. Zhang, Z. Hao, J. Mater. Chem. A 3 (2015) 8650–8658.
[3] L. Meng, M. Kanezashi, J. Wang, T. Tsuru, J. Membr. Sci. 496 (2015) 211–218.
[4] R.M. de Vos, H. Verweij, Science 279 (1998) 1710–1711.
[5] M. Kanezashi, M. Asaeda, J. Chem. Eng. Jpn 38 (2005) 908–912.
[6] A.K. Prabhu, S.T. Oyama, J. Membr. Sci. 176 (2000) 233–248.
[7] S. Battersby, S. Smart, B. Ladewig, S. Liu, M.C. Duke, V. Rudolph, J.C. Diniz da Costa, Sep. Purif. Technol. 66 (2009) 299–305.
[8] H.L. Castricum, A. Sah, R. Kreiter, D.H.A. Blank, J.F. Vente, J.E. ten Elshof, Chem. Commun. (2008) 1103–1105.
[9] R. Xu, J. Wang, M. Kanezashi, T. Yoshioka, T. Tsuru, Langmuir 27 (2011) 13996–13999.
[10] R. Xu, M. Kanezashi, T. Yoshioka, T. Okuda, J. Ohshita, T. Tsuru, ACS Appl. Mater. Interfaces 5 (2013) 6147–6154.
[11] R. Xu, S.M. Ibrahim, M. Kanezashi, T. Yoshioka, K. Ito, J. Ohshita, T. Tsuru, ACS Appl. Mater. Interfaces 6 (2014) 9357–9364.
[12] J. Ohshita, H. Muragishi, K. Yamamoto, T. Mizumo, M. Kanezashi, T. Tsuru, J. Sol-Gel Sci, Technology 73 (2015) 365–370.
[13] T. Mizumo, H. Muragishi, K. Yamamoto, J. Ohshita, M. Kanezashi, T. Tsuru, Appl. Organomet. Chem. 29 (2015) 433–438.
[14] K. Yamamoto, J. Ohshita, T. Mizumo, M. Kanezashi, T. Tsuru, Appl. Organomet. Chem. (2016) (in press).
[15] R.J.P. Corriu, J.J.E. Moreau, P. Thepot, M.W.C. Man, Chem. Mater. 4 (1992) 1217–1224.
[16] S.M. Ibrahim, R. Xu, H. Nagasawa, A. Naka, J. Ohshita, T. Yoshioka, M. Kanezashi, T. Tsuru, RSC Adv. 4 (2014) 23759–23769.
[17] T. Gunji, T. Shioda, K. Tsuchihira, H. Seki, T. Kajiwara, Y. Abe, Appl. Organomet. Chem. 24 (2010) 545–550.
[18] M. Kanezashi, T. Shioda, T. Gunji, T. Tsuru, AICHE J. 58 (2012) 1733–1743.
[19] M.M. Rahman, V. Filiz, S. Shishatskiy, C. Abetz, S. Neumann, S. Bolmer, M.M. Khan, V. Abetz, J. Membr. Sci. 437 (2013) 286–297.
[20] C.H. Worthley, K.T. Constantopoulos, M. Ginic-Markovic, E. Markovic, S. Clarke, J. Membr. Sci. 431 (2013) 62–71.
[21] P.G. Harrison, C. Hall, R. Kannengiesser, Main Group Met. Chem. 20 (1997) 515–530.
[22] The American Society for Testing and Materials (ASTM) D 3363–3392, Test Method for Film Hardness by Pencil Test.
[23] T. Tsuru, T. Hino, T. Yoshioka, M. Asaeda, J. Membr. Sci. 186 (2001) 257–265.
[24] T. Tsuru, Y. Takata, H. Kondo, F. Hirano, T. Yoshioka, M. Asaeda, Sep. Purif. Technol. 32 (2003) 23–27.
[25] T. Tsuru, K. Ogawa, M. Kanezashi, T. Yoshioka, Langmuir 26 (2010) 10897–10905.
[26] R. Xu, J. Wang, M. Kanezashi, T. Yoshioka, T. Tsuru, AICHE J. 59 (2013) 1298–1307.
[27] S.M. Ibrahim, H. Nagasawa, M. Kanezashi, T. Tsuru, J. Membr. Sci. 493 (2015) 515–523.
[28] K. Yamamoto, J. Ohshita, T. Mizumo, M. Kanezashi, T. Tsuru, Sep. Purif. Technol. 156 (2015) 396–402.
[29] J. Yu, C.H. Lee, W.H. Hong, Chem. Eng. Process. 41 (2002) 693–698.